Available online at www.sciencedirect.com
ScienceDirect
Geochimica et Cosmochimica Acta 71 (2007) 155–164
Geochimica
www.elsevier.com/locate/gca

Synthesis and properties of ammoniojarosites prepared with iron-oxidizing acidophilic microorganisms at 22–65 °C

Hongmei Wang [a,b,c], Jerry M. Bigham [b], Franklin S. Jones [b], Olli H. Tuovinen [a,*]

[a] Department of Microbiology, Ohio State University, 484 W. 12th Avenue, Columbus, OH 43210, USA
[b] School of Environment and Natural Resources, Ohio State University, 2021 Coffey Road, Columbus, OH 43210, USA
[c] School of Environmental Studies, China University of Geosciences, Wuhan 430074, People's Republic of China

Received 12 May 2006; accepted in revised form 1 September 2006

Abstract

Ammoniojarosite [$(NH_4,H_3O)Fe_3(OH)_6(SO_4)_2$], a poorly soluble basic ferric sulfate, was produced by microbiological oxidation of ferrous sulfate at pH 2.0–3.0 over a range of NH_4^+ concentrations (5.4–805 mM) and temperatures (22–65 °C). Ammoniojarosites were also produced by chemical (abiotic) procedures in parallel thermal (36–95 °C) experiments. At 36 °C, schwertmannite [ideally $Fe_8O_8(OH)_6(SO_4)$] was the only solid product formed at <10 mM NH_4^+ concentrations. Between 11.5 and 85.4 mM NH_4^+, a mixed product of ammoniojarosite and schwertmannite precipitated, as identified by X-ray diffraction. In excess of 165 mM NH_4^+, ammoniojarosite was the only solid phase produced. An increase in the incubation temperature using thermoacidophiles at 45 and 65 °C accelerated the formation of ammoniojarosite in culture solutions containing 165 mM NH_4^+. Both the biogenic and chemical ammoniojarosites were yellow (2Y–4Y in Munsell hue), low surface area (<1 m^2/g), well crystalline materials with average c_o and a_o unit cell parameters of 17.467 ± 0.048 Å and 7.330 ± 0.006 Å, respectively. Strong positive correlations were observed between unit cell axial ratios (c_o/a_o) and increasing synthesis temperature in both biotic and abiotic systems. All samples were N deficient compared to stoichiometric ammoniojarosite, and both chemical and X-ray data indicated partial replacement of NH_4^+ by H_3O^+ to form solid solutions with 0.14–0.24 mole H_3O^+ per formula unit. The morphology of the biogenic jarosites included aggregated discs, pseudo-cubic crystals and botryoidal particles, whereas the chemical specimens prepared at 36–95 °C were composed of irregular crystals with angular edges. Morphological information may thus be useful to evaluate environmental parameters and mode of formation. The data may also have application in predicting phase boundary conditions for Fe(III) precipitation in biogeochemical processes and treatment systems involving acid sulfate waters.

1. Introduction

Acidophilic chemolithotrophic microorganisms are well known for catalyzing the oxidation of pyrite and other Fe-sulfides (Olson et al., 2003; Rohwerder et al., 2003), resulting in the formation of acid ferric sulfate solutions that contribute to a variety of environmental problems. Under moderate to strongly acid conditions, ferric iron may precipitate in a variety of mineral forms, including both oxides and hydroxysulfates. These mixtures are usually poorly characterized, and the conditions for their biogenic formation have not been well defined. Ivarson (1973) was among the first to report that iron-oxidizing bacteria such as *Acidithiobacillus ferrooxidans* were capable of producing conditions that lead to jarosite formation [$MFe_3(OH)_6(SO_4)_2$], where M is usually K, Na, NH_4, or H_3O at ambient temperatures and pressures. Jarosite minerals have since been identified on numerous occasions in spent cultures of iron-oxidizing acidophiles (e.g., Lazaroff et al., 1985; Grishin et al., 1988; Sasaki et al., 1995, 1998; Sasaki, 1997; Daoud and Karamanev, 2006). Some members of the jarosite group are also commonly found in hyperacid natural environments, such as those associated with acid sulfate soils, acid rock drainage, and acid mine-impacted sediments (Bigham and Nordstrom, 2000).

* Corresponding author. Fax: +1 614 292 8120.
E-mail address: tuovinen.1@osu.edu (O.H. Tuovinen).

0016-7037/$ - see front matter © 2006 Elsevier Inc. All rights reserved.
doi:10.1016/j.gca.2006.09.001

The chemical composition of naturally occurring jarosites is often variable because of their tendency to form solid solutions that are not easily distinguished using standard diagnostic techniques (Alpers et al., 1989). Any direct effects of biogenetic pathways on jarosite crystal properties are also unknown. This question has been given new importance because of the recent identification of jarosite by the NASA rover Opportunity as part of the Mars Exploration Rover mission (Elwood Madden et al., 2004; Klingelhöfer et al., 2004).

Jarosite minerals are of commercial interest because the precipitation of these compounds has been widely adopted as a means of controlling impurities in hydrometallurgical circuits, especially in the Zn industry (Das et al., 1996). Research on commercial applications of jarosite technology has been focused on ammoniojarosite because of the relatively low cost of NH_4^+ salts (Dutrizac and Jambor, 2000). Jarosites are also of great importance in the bioleaching of metals where they may control ferric iron solubility, with monovalent cations available from nutrient salts and solubilization of accessory minerals. Precipitation of jarosites may cause diffusion barriers on mineral surfaces, thereby affecting the leaching rates. In bioleaching situations, jarosites strip silver from solution to form argentojarosite (Ahonen and Tuovinen, 1990; Sasaki et al., 1995). Ammonium ion, an important nitrogen source for microorganisms in bioleaching operations, may also be stripped from solution because of the formation of ammoniojarosite which then makes ammonium biologically unavailable in the process (Niemelä et al., 1994). Jarosites can act as sinks for monovalent cations in the interlayer positions of micas during weathering and bioleaching situations. This effect leads to mica alterations that can proceed as far as vermiculite or smectite formation (Bhatti et al., 1994; Bigham et al., 2001), thereby impacting the permeability of leach beds.

Natural ammoniojarosites are rare and are usually associated with carbonaceous beds where NH_4^+ originates from the decomposition of organic compounds, and the iron and sulfate are derived from the oxidation of contaminant pyrite (FeS_2) (Odum et al., 1982). No information is available from the literature regarding the range of NH_4^+ concentrations in natural systems where ammoniojarosite typically forms.

The objective of this study was to produce biogenic ammoniojarosites over a range of NH_4^+ concentrations and temperatures ranging from 22 to 65 °C using iron-oxidizing bacteria and thermophilic archaea to oxidize ferrous sulfate to ferric iron in different formulations of acid mineral salts solutions. The precipitates collected were used to (1) define experimental conditions for pure ammoniojarosite formation and (2) examine the effects of incubation conditions on structural and morphological properties of the products. Chemical syntheses of ammoniojarosite from ferric sulfate solutions were also conducted with temperature as a variable for comparative purposes. Jarosites and other hydroxysulfates control the solubility of ferric iron in many bioleaching and acid mine drainage systems; therefore, information on their formation as pure phases or solid solution series has application in biogeochemical modeling of Fe^{3+}.

2. Materials and methods

2.1. Cultures of microorganisms

Iron-oxidizing bacteria and archaea were used for ferrous sulfate oxidation. For mesophilic experiments at 22 ± 2 °C (room temperature) and $36–37 \pm 2$ °C, the iron-oxidizers were an enrichment culture of *A. ferrooxidans* (designated MAF) obtained from the sediments of a constructed wetland treating coal-mine drainage. This wetland system was situated in Carbondale, Ohio and had an oxic surface layer comprised of Fe(III) precipitates with *A. ferrooxidans* as the dominant bacterium (Gagliano et al., 2004; Nicomrat et al., 2006a,b). Iron-oxidizing bacteria were enriched in a mineral salts solution (MSS) comprised of 1.6 mM $MgSO_4{\cdot}7H_2O$, 3.0 mM $(NH_4)_2SO_4$, 2.9 mM KH_2PO_4, and 120 mM $FeSO_4{\cdot}7H_2O$/l at pH 2.0–2.5 for several passages prior to these experiments. For the elevated temperature range (45 and 65 °C), two thermophilic cultures were used. No effort was made to incubate these cultures at their previously reported optimal temperatures since these microorganisms were only used to oxidize ferrous iron for the subsequent precipitation of jarosite. *Sulfolobus metallicus*, an iron-oxidizing archaeon, was used for ferrous sulfate oxidation at 45 °C. The culture was obtained from Dr. E. Börje Lindström, Department of Molecular Biology, Umeå University, Umeå, Sweden (UmU) and routinely maintained in MSS. Thus the thermophilic *S. metallicus* was grown in this study under moderately thermophilic conditions. Thermophilic bacteria, comprising a mixed culture designated MT, were obtained from Dr. Mark Dopson, Department of Molecular Biology, UmU. The MT culture was previously characterized as a moderately thermophilic consortium. The culture has been reported to contain *Acidithiobacillus caldus* and *Sulfobacillus* spp. as dominant bacteria, based on DGGE analysis of MT after growth at 45 °C (Dopson and Lindström, 2004), but in the present work its iron-oxidizing population was selected for by maintaining the culture with ferrous sulfate at 65 °C in MSS. Since the culture was only used to oxidize ferrous sulfate for jarosite experiments at 65 °C, no effort was made to identify the predominant organisms in this thermophilic consortium.

For ammoniojarosite experiments (Table 1), the MSS medium was reformulated to avoid the precipitation of K-jarosite, which is formed even at low concentrations of K^+. The modified mineral salts medium contained 1.6 mM $MgSO_4{\cdot}7H_2O$, 5.4 mM $NH_4H_2PO_4$ and 120 mM $FeSO_4{\cdot}7H_2O$ in 4.05 mM H_2SO_4. The initial pH was adjusted with H_2SO_4 to 2.3–2.6. In one experiment, greater ammonium levels were obtained by the addition of supplemental $(NH_4)_2SO_4$. In a second experiment, the concentration of

Table 1
Experimental conditions

Sample code	Temperature (°C)	Culture	$[NH_4^+]$ (mM)	Final pH
NH_4^+ concentration experiment				
B1	36	MAF	5.4	2.0
B2	36	MAF	9.4	2.0
3.5.9	36	MAF	11.5	2.2
B3	36	MAF	25.4	2.0
B4	36	MAF	45.4	2.0
3.5.11	36	MAF	85.4	2.5
3.5.12	36	MAF	165	2.4
3.5.13	36	MAF	245	2.6
3.5.14	36	MAF	325	2.6
3.5.16	36	MAF	565	2.7
3.6.8	36	MAF	805	3.1
Biotic temperature experiment				
3.5.8	22	MAF	165	2.2
R.2.3	36	MAF	165	2.2
Th.1	45	*Sulfolobus*	165	2.2
Th.6	65	*MT*	165	2.0
Abiotic temperature experiment				
6.5	36	None	200	2.1
6.6	65	None	200	1.8
6.3	95	None	2000	—

NH_4^+ was set at 165 mM, and oxidation was completed at 22 ± 2 °C, 36 ± 2 °C, 45 ± 1 °C, and 65 ± 1 °C using test cultures growing with Fe^{2+} as the substrate. All cultures (100 ml) were incubated in 250 ml shake flasks under aerobic conditions. Soluble iron was completely oxidized within a couple of days, but any precipitates were aged by extending the incubation for 1 week unless otherwise specified.

Mesophilic cultures growing with 120 mM Fe^{2+} reached a density of about 3×10^8 cells/ml. All cultures were grown with CO_2 in ambient air as the source of carbon, and no organic compounds were included in the media. Fully grown cultures remained active for months in the spent media.

Exact abiotic duplication of all biotic jarosite samples was not attempted because of the large number of biological samples examined for this study and because synthetic (abiotic) jarosites have already been characterized in the literature. Therefore, abiotic samples were primarily used to extend the temperature range of synthesis and were not controls in the traditional sense. Abiotic jarosite samples were prepared with ferric sulfate and ammonium sulfate at 36 °C (prepared in 120 mM Fe^{3+} and 200 mM NH_4^+; contact time 27 days), 65 °C (120 mM Fe^{3+} and 200 mM NH_4^+; contact time 8 days), and 95 °C (75 mM Fe^{3+} and 2000 mM NH_4^+; contact time 24 h). The iron and ammonium concentrations for the 95 °C synthesis were based on Dutrizac and Kaiman (1976). All precipitates were collected by centrifugation, washed twice with 5 mM H_2SO_4, and dried at 65 °C for 10 h before analysis. Jarosites are insoluble in weak sulfuric acid, and rapid washing had no detectable effect on the samples (no surface pitting, and no removal of poorly crystalline phases). Two reference hydronium jarosites (abiotic) were a gift from Dr. John E. Dutrizac, Mining and Mineral Sciences Laboratories, Canada Centre for Minerals and Technology, Ottawa, Ont., Canada.

2.2. Analytical methods

Powdered biogenic and abiotic precipitates were characterized by X-ray diffraction (XRD) using CuKα radiation and a Philips PW 1316/90 diffractometer equipped with a diffracted-beam monochromator and a 1° divergence slit. All samples were initially scanned from 3° to 80° 2θ with a step interval of 0.05° 2θ and 4 s counting time. Those materials containing pure ammoniojarosite were subsequently re-scanned with a shorter step interval (0.02° 2θ) and longer (10 s) dwell time. The resulting XRD data were analyzed using Jade version 3.1 from Materials Data, Inc. with the settings summarized in Table 2.

For scanning electron microscopy (SEM), samples were mounted on Al-stubs with double-sided carbon tabs and coated with a thin layer of gold in a Pelco Model 3 Sputter 91000 coater. Images were collected with a Philips XL 30 instrument operated at 15 kV accelerating voltage.

For elemental analysis, samples were dried at 110 °C and completely dissolved in 6 M HCl over a 48 h period. Aliquots were then diluted 1:60 with deionized water, and total Fe content was determined by atomic absorption spectroscopy with a Varian SpectrAA instrument at 372.0 nm and a slit width of 0.2 nm. Total S analyses were carried out using a LECO Model 518 instrument with K-iodate titration of SO_2 evolved by combustion of samples at 900 °C. Total C and N analyses were carried out with an NC 2100 Soil ThermoQuest instrument using 20 mg samples. All analytical standards were per manufacturers' directions.

Specific surface areas were measured (Brunauer–Emmet–Teller method) using a Micromeritics DeSorb 2300A surface area analyzer with N_2 as the adsorbate. Colors of the dried powders were determined with a Minolta

Table 2
Parameters and settings (Jade version 3.1, Materials Data Inc.) for analysis of X-ray diffraction patterns

Parameter	Setting
Peak search	
Filter length points	7
Intensity cutoff (%)	0.5
Threshold sigma	0.5
Peak position	By summit
Kα2	Screened out
Unit cell refinement	
Zero offset correction	None
Sample displacement correction	None
Least squares weighting	None
Cell type	Hexagonal primitive
Space group	R-3m(166)
Error window	0.3

CR-300 chromameter and were expressed using standard Munsell notations.

3. Results and discussion

3.1. Effect of NH_4^+ concentration on biogenic precipitates

The bacterial oxidation of solutions containing <10 mM NH_4^+ (samples B1 and B2) yielded schwertmannite, ideally $Fe_8O_8(OH)_6SO_4$, as the only identifiable product of Fe(II) oxidation and hydrolysis (Table 3). Schwertmannite is a poorly crystalline phase that has frequently been identified in mineral precipitates from acid sulfate waters (Bigham and Nordstrom, 2000). The materials produced in this study gave characteristic XRD profiles (Fig. 1a) consisting of eight broad, overlapping peaks. Morphological properties were also typical of schwertmannite, with most particles occurring as rounded aggregates, 1–2 μm in diameter, that were composed of thin, needle-like crystals giving a "pin-cushion" appearance under the SEM (Fig. 2a). Although the morphology and XRD profiles were typical of schwertmannite, colors were redder (6.5 YR vs. 10 YR) and surface areas were less (10 vs 200 m^2/g) (Table 3) than previously observed for either synthetic or natural specimens (Bigham and Nordstrom, 2000). In addition, Bigham et al. (1992) reported that schwertmannite usually precipitates in the pH range of 3.0–4.0. In this study, schwertmannite was formed at pH values as low as 2.0. Recently, Majzlan and Myneni (2005) reported that schwertmannite rather than hydronium jarosite was the phase that controlled the solubility and short-term availability of Fe(III) and SO_4^{2-} in acid sulfate waters deficient in other monovalent cations. This observation is consistent with our findings in that schwertmannite was always formed when monovalent cations other than hydronium (i.e., K^+, Na^+, NH_4^+) were limiting.

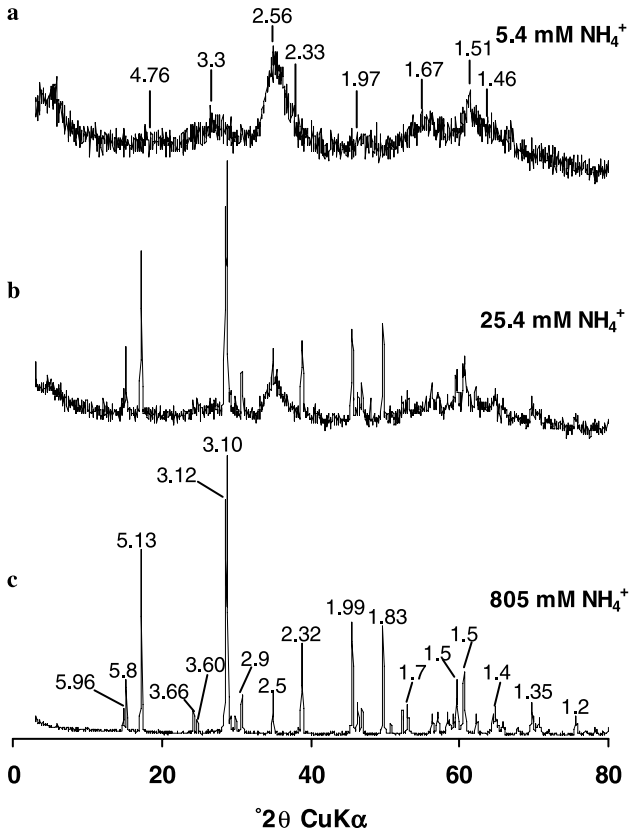

Fig. 1. Representative XRD patterns of biogenic precipitates from the NH_4^+ concentration series. (a) Sample B1 (schwertmannite) prepared with 5.4 mM NH_4^+, (b) sample B3 (schwertmannite + ammonium jarosite) prepared with 25.4 mM NH_4^+, and (c) sample 3.6.8 (ammoniojarosite) prepared with 805 mM NH_4^+. Numerical values are diagnostic peak positions in Å units.

Table 3
Mineral composition, color, and surface area of precipitates (Sh, Schwertmannite; Aj, Ammoniojarosite; I.S., insufficient sample)

Sample	Treatment	Mineral composition	Munsell color	Surface area (m^2/g)
NH_4^+ concentration experiment				
B1	5.4 mM NH_4^+	Sh	6.3YR 4.3/8.6	10.3
B2	9.4 mM NH_4^+	Sh	6.4YR 4.5/8.5	12.1
3.5.9	11.5 mM NH_4^+	Sh + Aj	8.4YR 6.6/7.9	
B3	25.4 mM NH_4^+	Sh + Aj	6.1YR 4.4/6.6	I.S.
B4	45.4 mM NH_4^+	Sh + Aj	7.0YR 4.6/6.6	I.S.
3.5.11	85.4 mM NH_4^+	Sh + Aj	8.8YR 6.7/8.4	13.8
3.5.12	165 mM NH_4^+	Aj	2.6Y 7.3/6.6	0.57
3.5.13	245 mM NH_4^+	Aj	2.3Y 7.2/7.0	0.35
3.5.14	325 mM NH_4^+	Aj	3.2Y 7.7/6.4	0.59
3.5.16	565 mM NH_4^+	Aj	2.5Y 7.2/6.9	0.30
3.6.8	805 mM NH_4^+	Aj	3.0Y 7.6/6.5	
Biotic temperature experiment				
3.5.8	22 °C	Aj	2.4Y 7.2/6.2	0.70
R.2.3	36 °C	Aj	3.2Y 7.7/6.4	0.62
Th.1	45 °C	Aj	3.2Y 7.6/6.6	0.91
Th.6	65 °C	Aj	1.9Y 7.2/7.1	0.64
Abiotic temperature experiment				
6.5	36 °C	Aj	2.1Y 6.9/6.0	0.46
6.6	45 °C	Aj	2.0Y 7.1/5.3	0.34
6.3	95 °C	Aj	3.8Y 8.3/5.2	1.11

At solution concentrations in the range of 11.5–85.4 mM NH_4^+ (samples B3, B4, 3.5.9, and 3.5.11), mixed precipitates of schwertmannite and ammoniojarosite were produced (Table 3). The sharp, well-resolved peaks of ammoniojarosite were superimposed on the broad peaks of schwertmannite in XRD traces (Fig. 1b). SEM micrographs commonly showed schwertmannite aggregates coating cubic or octahedral ammoniojarosite crystals (Fig. 2b), and suggested that schwertmannite was precipitated after the formation of ammoniojarosite. This observation is not conclusive because no attempt was made to monitor NH_4^+ consumption and thereby confirm a preferential order of precipitation.

Precipitate colors became yellower as jarosite contents increased (Table 3). When NH_4^+ was present in the media at concentrations of 165 mM or greater, the canary-yellow precipitates (2.5–3.2 Y) produced by biological Fe oxidation consisted of dense aggregates of botryoidal and

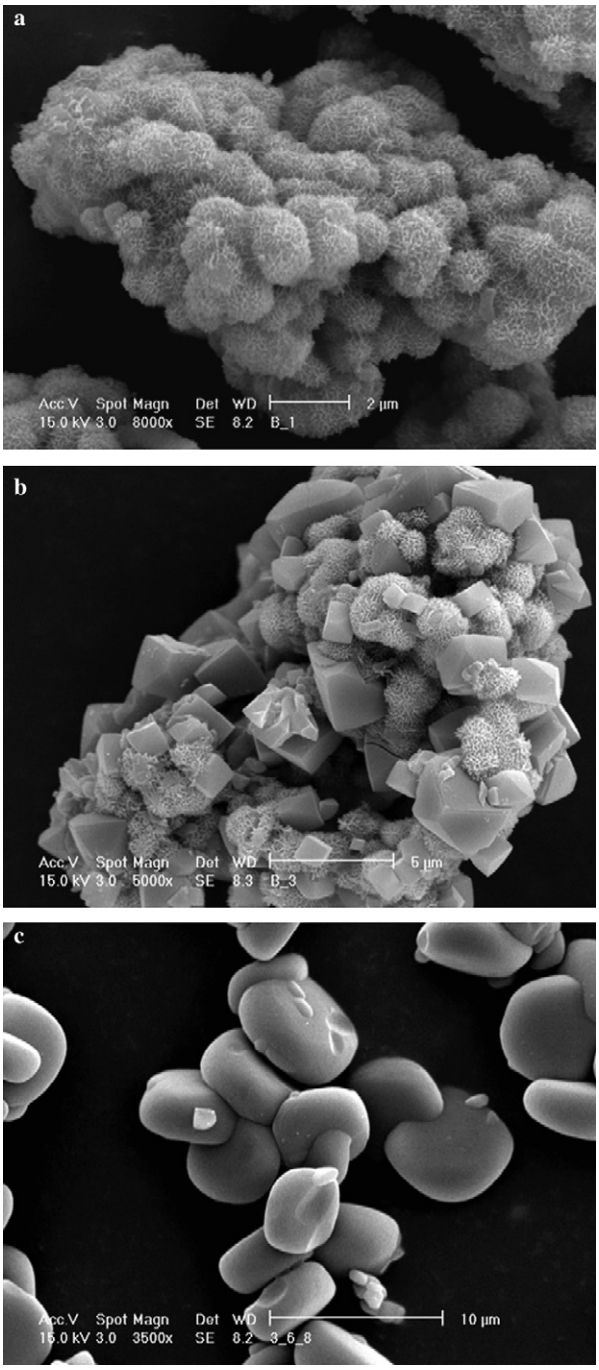

Fig. 2. SEM micrographs of Fe(III) precipitates. (a) Sample B1 (schwertmannite) prepared with 5.4 mM NH_4^+, (b) sample B3 (schwertmannite + ammonium jarosite) prepared with 25.4 mM NH_4^+, and (c) sample 3.6.8 (ammoniojarosite) prepared with 805 mM NH_4^+.

disc-shaped crystals (Fig. 2c) with surface areas of only 0.3–0.6 m^2/g (Table 3). Chemical analyses demonstrated surpluses of Fe ($\Delta Fe = 1.0$–2.8%) and deficiencies of S ($\Delta S = -0.26\%$ to -0.88%) and N ($\Delta N = -0.56\%$ to -0.69%) compared to stoichiometric ammoniojarosite (Table 4). These trends could be explained by impurities of schwertmannite or other foreign compounds in the samples, but XRD results showed low background intensities and yielded no anomalous peaks indicative of contaminants.

As noted previously, jarosites may form solid solutions with the monovalent cations, Na^+, K^+, H_3O^+, and NH_4^+, and pure end members are rarely, if ever, found in nature (Alpers et al., 1989). In this study, salts of Na^+ and K^+ were excluded from the bacterial growth media, but the replacement of NH_4^+ with 0.14–0.24 mole H_3O^+ per formula unit could account for the observed deficiencies of N. Similar substitution levels have been reported for K–Na–H_3O solid solution jarosites by Alpers et al. (1989) and Drouet and Navrotsky (2003). In the current study, there was a strong positive correlation between concentration of NH_4^+ in the growth media and N content of the ammoniojarosites suggesting that even greater N contents could be achieved with solution concentrations in excess of 805 mM NH_4^+ (Fig. 3a).

Both ammoniojarosite and hydronium jarosite belong to the trigonal crystal system. For ammoniojarosite, $a_o = 7.327$ and $c_o = 17.50$ ($c_o/a_o = 2.397$) (Smith and Lampert, 1973); whereas, $a_o = 7.36$ and $c_o = 17.0$ ($c_o/a_o = 2.310$) for hydronium jarosite. Variations in the c_o of jarosites are related to the size of the monovalent cation (Stoffregen et al., 2000), and Vegard's Law states that the lattice parameters in a solid solution vary linearly with increasing concentration of end-member species (Vegard and Dale, 1928). Thus, as NH_4^+ content increases with respect to H_3O^+ in a solid-solution jarosite, the ratio c_o/a_o should increase. While the correlation between c_o/a_o and N content was positive, the relationship was poor ($R^2 = 0.20$) (Fig. 3b) indicating that the NH_4^+/H_3O^+ cation ratio had little influence on the unit cell lengths of materials synthesized under near ambient conditions of temperature and pressure.

3.2. Effect of temperature on biotic and abiotic precipitates

Although precipitation rates were not measured, there was clearly a positive correlation between temperature and the rate of ammoniojarosite formation at comparable ammonium concentrations and pH values. About 2 months were required for ammoniojarosite to form at room temperature; whereas only 7 days were needed at 36 °C and higher. The quantity of precipitate formed also increased with increasing temperature. Direct measurements showed that conversion of Fe(II) to Fe(III) in the biotic series was always complete within 7 days, so rate and quantity of ammoniojarosite formation were not influenced by the rate of Fe oxidation in these experiments.

X-ray diffraction results showed that all precipitates formed as a result of iron oxidation by mesophilic and thermophilic acidophiles over the temperature range of 22–65 °C and in the presence of at least 165 mM NH_4^+ were well crystalline ammoniojarosites (Fig. 4a–c). The XRD profiles were visually indistinguishable from those obtained from abiotic specimens that were produced at elevated temperatures by hydrolysis of Fe(III) sulfate solutions with comparable or greater NH_4^+ concentrations (Fig. 4d). In the biotic series, there was a clear tendency for c_o to

Table 4
Unit cell parameters and chemical composition of ammoniojarosites

Specimen	Treatment	a_o (Å)	e.s.d. (a_o) (Å)	c_o (Å)	e.s.d. (c_o) (Å)	c_o/a_o	N (%)	Fe (%)	S (%)	ΔN^* (%)	ΔFe^* (%)	ΔS^* (%)
NH_4^+ concentration series												
3.5.12	165 mM NH_4^+	7.32981	0.00098	17.44031	0.00265	2.379	2.23	37.2	12.45	−0.69	2.2	−0.88
3.5.13	245 mM NH_4^+	7.33072	0.00097	17.42286	0.00212	2.377	2.23	37.2	12.91	−0.69	2.2	−0.42
3.5.14	325 mM NH_4^+	7.31312	0.00120	17.44088	0.00208	2.385	2.34	37.8	13.07	−0.58	2.8	−0.26
3.5.16	565 mM NH_4^+	7.33059	0.00085	17.40804	0.00241	2.375	2.36	37.2	12.70	−0.56	2.2	−0.63
3.6.8	805 mM NH_4^+	7.33201	0.00033	17.47504	0.00092	2.383	2.51	36.0	12.71	−0.41	1.0	−0.62
Biotic temperature series												
3.5.8	22 °C	7.33372	0.00106	17.44604	0.00233	2.379	2.23	34.0	13.35	−0.69	−1.0	0.02
R.2.3	36 °C	7.33455	0.00058	17.47868	0.00149	2.383	2.26	37.2	12.93	−0.69	2.2	−0.40
Th.1	45 °C	7.33127	0.00064	17.55438	0.00152	2.394	2.34	37.2	11.88	−0.58	2.2	−1.45
Th.6	65 °C	7.32974	0.00084	17.56150	0.00225	2.396	2.35	34.4	11.88	−0.56	−0.6	−1.45
Abiotic temperature series												
6.5	36 °C	7.32990	0.00090	17.43491	0.00232	2.379	2.17	37.2	13.70	−0.75	2.2	0.37
6.6	65 °C	7.32938	0.00106	17.46088	0.00294	2.382	2.10	33.6	14.07	−0.82	−1.4	0.74
6.3	95 °C	7.33330	0.00088	17.48647	0.00228	2.385	2.42	37.2	13.11	−0.50	2.2	−0.22
Ideal		7.32		17.5		2.397	2.92	35.0	13.33			

* Deficiency or excess compared to ideal formula for ammoniojarosite.

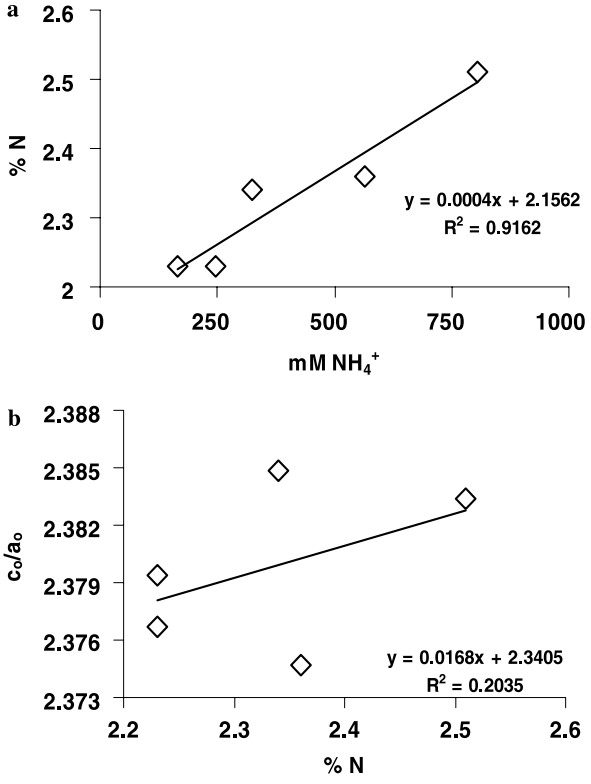

Fig. 3. (a) Relationship between N content of biotic ammoniojarosites formed at 36 °C and the concentration of NH_4^+ in the growth medium. (b) Influence of N content on the unit cell axial ratio (c_0/a_o) of biotic ammoniojarosites formed at 36 °C.

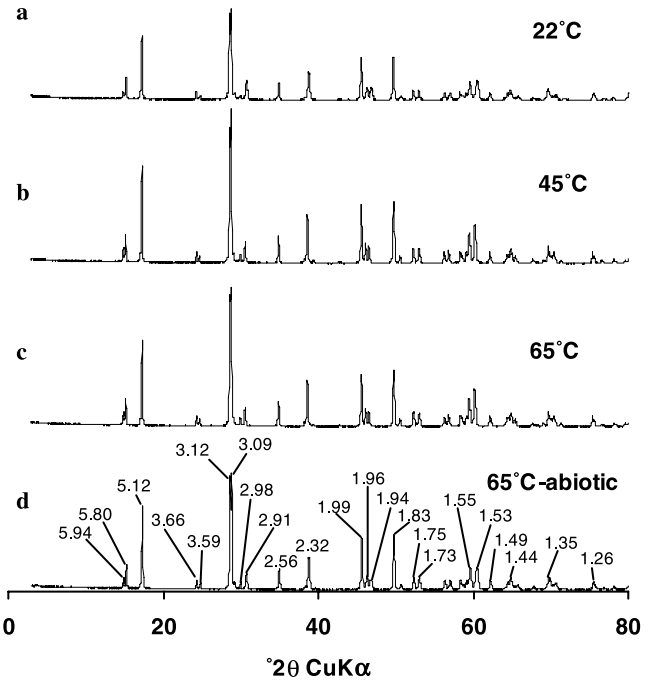

Fig. 4. Representative XRD patterns of ammoniojarosite samples. (a) Biogenic precipitate formed at 22 °C (sample 3.5.8), (b) biogenic precipitate formed at 45 °C (sample Th.1), (c) biogenic precipitate formed at 65 °C (sample Th.6), and (d) abiotic precipitate formed at 45 °C (sample 6.6). Numerical values are diagnostic peak positions in Å units.

increase with increasing temperature (and N content) (Table 4) yielding strong correlations between c_o/a_o and both the synthesis temperature and %N (Fig. 5a and b). A similar positive relationship existed for c_o/a_o with respect to temperature for the abiotic samples (Fig. 5c), but the correlation with N content was surprisingly poor (Fig. 5a). Nitrogen content of the biotic products was, on average, higher than the abiotic precipitates and was perhaps a result of contributions from microbial biomass retained in the samples. Fe and S contents showed no clear trends with respect to temperature or the ideal formulation for ammoniojarosite (Table 4).

Plots of c_o/a_o vs unit cell volumes calculated from the XRD cell refinements showed that cell volumes increased

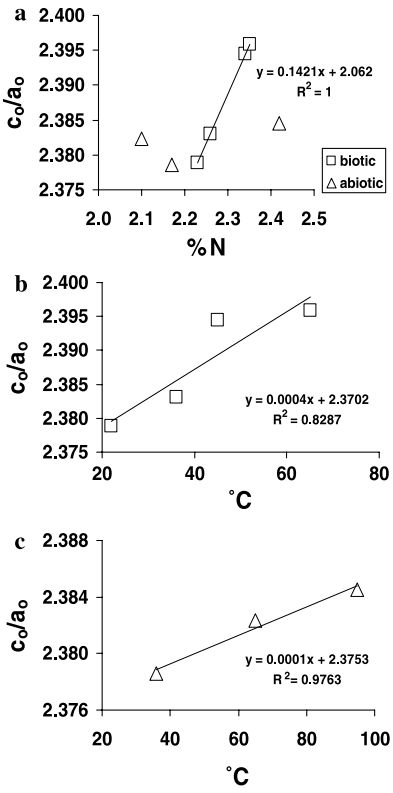

Fig. 5. Relationship between the unit cell axial ratio (c_0/a_o) of temperature series ammoniojarosites as related to: (a) the solid-phase N content, (b) the temperature of formation for biotic samples, and (c) the temperature of formation for abiotic samples.

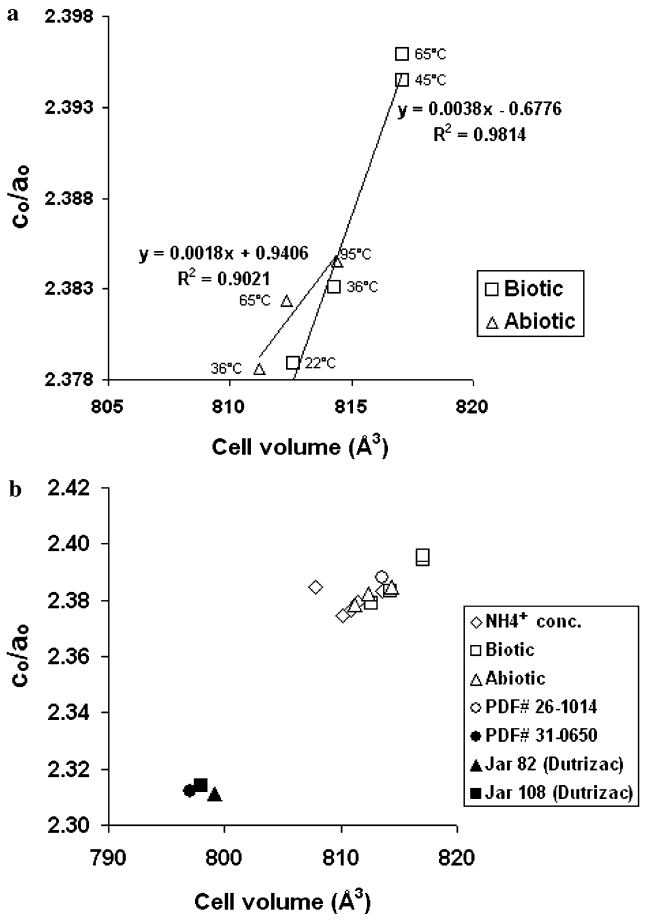

Fig. 6. Relationship between axial ratio (c_0/a_o) and the unit cell volume of (a) the temperature series ammoniojarosites, and (b) all jarosites prepared in this study. Reference powder diffraction file (PDF) data include: PDF# 26-1014 (abiotic ammoniojarosite); PDF #31-0650 (abiotic hydronium jarosite). Jar 82 and Jar 108 are experimental data for hydronium jarosite samples provided by Dr. J.E. Dutrizac.

with increasing temperature, and the increases were anisotropic with little change in a_o relative to c_o (Fig. 6a). The cell volumes obtained in this study compared reasonably well with those of reference ammoniojarosite and were distinctly different from both experimental and reported data for hydronium jarosite (Fig. 6b). Nevertheless, all products were deficient in N compared to stoichiometric ammoniojarosite, and the deficiency tended to decrease with increasing temperature (Table 4). Brophy and Sheridan (1965) reported that the amount of H_3O^+ in the structure of synthetic jarosites decreased with increasing temperature and pressure. Physical evidence of H_3O^+ substitution for NH_4^+ in the biotic and abiotic temperature series was provided by the intense (0 2 1) and (1 1 3) peaks in XRD traces (Fig. 7a and b). These peaks are more closely spaced in ammoniojarosite than in hydronium jarosite. Consequently, small but linear decreases in $\Delta 2\Theta_{(113-021)}$ with increasing temperature are consistent with temperature-induced reductions in hydronium substitution (Fig. 8).

Colors of both the biotic and abiotic products were fairly uniform with hues, values, and chromas ranging from 1.9 to 3.8Y, 7.1 to 8.3, and 5.2 to 7.1, respectively (Table 3). Although specific surface areas were comparable to those obtained for pure ammoniojarosites in the NH_4^+ concentration experiment (<1 m^2/g), clear differences in particle morphology were observed in response to temperature and, perhaps, aging while in contact with the solution phase. Aggregates of disc-shaped crystals were produced at room temperature (Fig. 9a), whereas biotic specimens precipitated at 45 and 65 °C formed rosette-shaped particles having diameters in the order of 10–20 μm (Fig. 9b and c). Abiotic precipitates produced at elevated temperatures were less aggregated and were composed of angular particles with diameters in the order of 10 μm (Fig. 9d). The strong aggregation observed with biotic specimens may be attributable to cellular materials acting to bind individual mineral particles as previously suggested by Sasaki and Konno (2000). However, strands of extracellular polymers or cell fragments were not apparent in SEM micrographs, and jarosite crystal surfaces were clean and free of cell debris. Indirect effects on mineral properties caused by cellular binding materials may or may not be distinguishable from the direct influence that microorganisms could have on the rate or pathway of reaction. Answers to these questions would require comparisons of systems with living vs. intact but other-

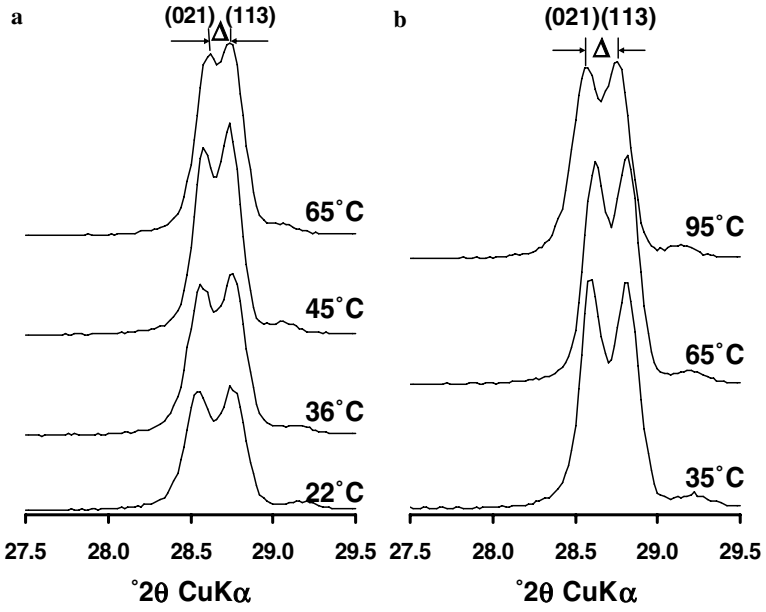

Fig. 7. Stacked XRD patterns for (a) biotic and (b) abiotic specimens showing the relative positions of the (021) and (113) peaks as a function of synthesis temperature.

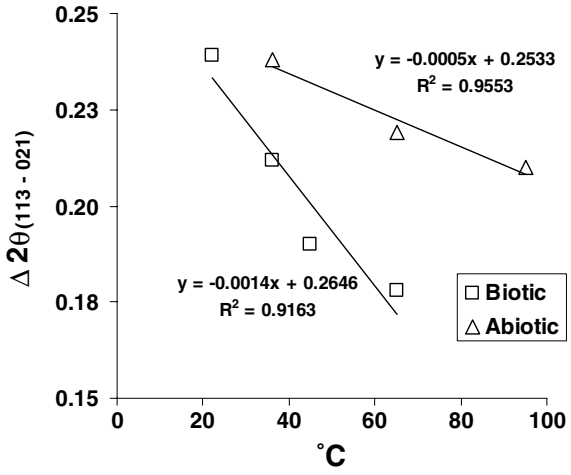

Fig. 8. Spacing difference for (021) and (113) peaks as a function of temperature for biotic and abiotic ammoniojarosites.

wise inactive bacteria. In this regard, the jarosite solid solution system in this study is very different from the aggregate development of Fe(III) oxyhydroxides that involves biomineralization with bacterial stalks and other cellular nucleation sites, characterized in samples from mine sites with tufts and other congregations of microbial occurrence (Banfield et al., 2000; Chan et al., 2004).

3.3. Conclusions

In previous studies of jarosite biosynthesis, *A. ferrooxidans* cells were removed from the media after partial or complete iron oxidation had occurred, and jarosite-directing cations (e.g., K, Na, NH_4) were then added to obtain mineral products from spent culture solutions (Lazaroff et al., 1982, 1985; Sasaki et al., 1995, 1998). In natural environments, jarosite-determining cations are usually part of the geochemical system during iron oxidation, and mineral phases are thus produced in a competitive manner as determined by both thermodynamic and kinetic factors (Kawano and Tomita, 2001). We established that schwertmannite was the favored product of biological Fe^{2+} oxidation at 22 and 36 °C, even at pH values as low as 1.9, when the NH_4^+ concentration was less than 10 mM and other alkali cations were excluded from the system. In the range of 11.5–85.4 mM NH_4^+, mixed schwertmannite–ammoniojarosite precipitates were formed, and ammoniojarosite was the sole product only when NH_4^+ exceeded 165 mM. Such elevated concentrations of NH_4^+ would not likely be found in most natural environments that are otherwise conducive to jarosite formation. Parallel experiments were not run in the thermophilic temperature range with ammonium concentration as a variable.

The solid solution series of biological ammoniojarosites prepared in this study could not be consistently distinguished from abiotic samples on the basis of structure (powder XRD), chemical composition, color or surface area. The biological specimens did, however, consist of more rounded or disk-shaped particles than the corresponding chemical products. We conclude that the role of microorganisms in the crystallization of ammoniojarosite involves primarily the catalysis of iron oxidation at low pH, and that the formation of mineral species under hyperacid conditions in nature is otherwise controlled by geochemical factors.

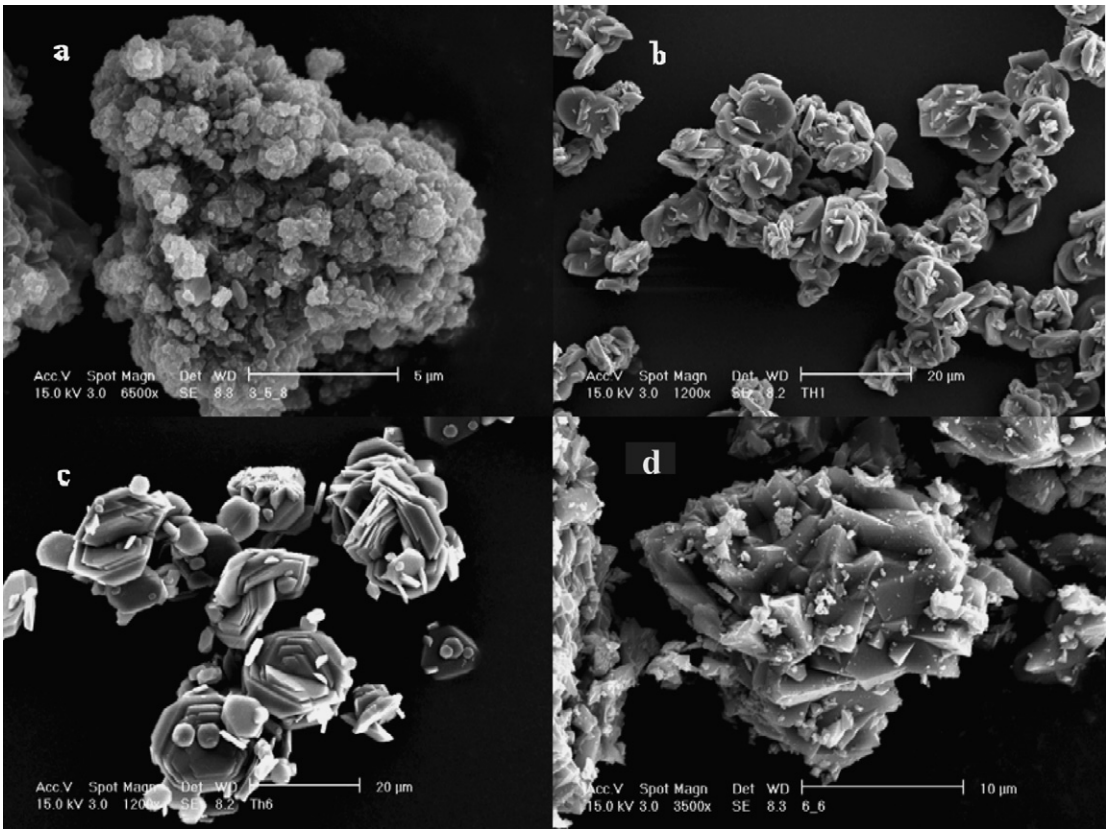

Fig. 9. SEM micrographs of ammoniojarosite samples. (a) Biogenic precipitate formed at 22 °C (sample 3.5.8), (b) biogenic precipitate formed at 45 °C (sample Th.1), (c) biogenic precipitate formed at 65 °C (sample Th.6), and (d) abiotic precipitate formed at 45 °C (sample 6.6).

Acknowledgments

We thank M. Dopson and E.B. Lindström for the MT and *Sulfolobus* cultures, J.E. Dutrizac for the hydronium jarosite samples, and D.E. Fulton, Molecular and Cellular Imaging Center of the Ohio Agricultural Research and Development Center, for advice on scanning electron microscopy. H. Wang was supported by the Ministry of Education, Natural Science Foundation project 40525008, Hubei Province project 2003500216-29, and the Bio- and Environmental Geology Laboratory in the China University of Geosciences, People's Republic of China. Partial salary and research support were provided to F.S. Jones and J.M. Bigham by state and federal funds appropriated to the Ohio Agricultural Research and Development Center. We thank three anonymous reviewers and Associate Editor J.B. Fein for insightful suggestions that were helpful in improving the manuscript.

Associate editor: Jeremy B. Fein

References

Ahonen, L., Tuovinen, O.H., 1990. Silver catalysis of the bacterial leaching of chalcopyrite-containing ore material in column reactors. *Miner. Eng.* **5**, 437–445.

Alpers, C.N., Nordstrom, D.K., Ball, J.W., 1989. Solubility of jarosite solid solutions precipitated from acid mine waters, Iron Mountain, California, U.S.A. *Sci. Géol. Bull.* **42**, 281–298.

Banfield, J.F., Welch, S.A., Zhang, H., Ebert, T.T., Penn, R.L., 2000. Aggregation-based crystal growth and microstructure development in natural iron oxyhydroxide biomineralization products. *Science* **289**, 751–754.

Bhatti, T.M., Bigham, J.M., Vuorinen, A., Tuovinen, O.H., 1994. Alteration of mica and feldspar associated with the microbiological oxidation of pyrrhotite and pyrite. In: Alpers, C.N., Blowes, D.W. (Eds.), *Environmental Geochemistry of Sulfide Oxidation*. American Chemical Society, Washington, DC, pp. 90–105.

Bigham, J.M., Nordstrom, D.K., 2000. Iron and aluminum hydroxysulfates from acid sulfate waters. *Rev. Mineral. Geochem.* **40**, 351–403.

Bigham, J.M., Schwertmann, U., Carlson, L., 1992. Mineralogy of precipitates formed by the biogeochemical oxidation of Fe(II) in mine drainage. In: Skinner, H.C.W., Fitzpatrick, R.W. (Eds.), *Biomineralization of Iron and Manganese—Modern and Ancient Environments*. Catena Verlag, Reiskirchen, Germany, pp. 219–232.

Bigham, J.M., Bhatti, T.M., Vuorinen, A., Tuovinen, O.H., 2001. Dissolution and structural alteration of phlogopite mediated by proton attack and bacterial oxidation of ferrous iron. *Hydrometallurgy* **59**, 301–309.

Brophy, G.P., Sheridan, M.F., 1965. Sulfate studies. II. Solid solution between alunite and jarosite. *Am. Mineral.* **47**, 112–126.

Chan, C.S., De Stasio, G., Welch, S.A., Girasole, M., Frazer, B.H., Nesterova, M.V., Fakra, S., Banfield, J.F., 2004. Microbial polysaccharides template assembly of nanocrystal fibers. *Science* **303**, 1656–1659.

Daoud, J., Karamanev, D., 2006. Formation of jarosite during Fe^{2+} oxidation by *Acidithiobacillus ferrooxidans*. *Miner. Eng.* **19**, 960–967.

Das, G.K., Acharya, S., Anand, S., Das, R.P., 1996. Jarosites: a review. *Miner. Process. Extract. Metall. Rev.* **16**, 185–210.

Dopson, M., Lindström, E.B., 2004. Analysis of community composition during moderately thermophilic bioleaching of pyrite, arsenical pyrite, and chalcopyrite. *Microb. Ecol.* **48**, 19–28.

Drouet, C., Navrotsky, A., 2003. Synthesis, characterization, and thermochemistry of K–Na–H_3O jarosites. *Geochim. Cosmochim. Acta* **67**, 2063–2076.

Dutrizac, J.E., Jambor, J.L., 2000. Jarosites and their application in hydrometallurgy. *Rev. Mineral. Geochem.* **40**, 402–452.

Dutrizac, J.E., Kaiman, S., 1976. Synthesis and properties of jarosite-type compounds. *Can. Mineral.* **14**, 151–158.

Elwood Madden, M.E., Bodnar, R.J., Rimstidt, J.D., 2004. Jarosite as an indicator of water-limited chemical weathering on Mars. *Nature* **431**, 821–823.

Gagliano, W.B., Brill, M.R., Bigham, J.M., Jones, F.S., Traina, S.J., 2004. Chemistry and mineralogy of ochreous sediments in a constructed mine drainage wetland. *Geochim. Cosmochim. Acta* **68**, 2119–2128.

Grishin, S.I., Bigham, J.M., Tuovinen, O.H., 1988. Characterization of jarosite formed upon bacterial oxidation of ferrous sulfate in a packed-bed reactor. *Appl. Environ. Microbiol.* **54**, 3101–3106.

Ivarson, K.C., 1973. Microbiological formation of basic ferric sulfates. *Can. J. Soil Sci.* **53**, 315–323.

Kawano, M., Tomita, K., 2001. Geochemical modeling of bacterially induced mineralization of schwertmannite and jarosite in sulfuric acid spring water. *Am. Mineral.* **86**, 1156–1165.

Klingelhöfer, G., Morris, R.V., Bernhardt, B., Schröder, C., Rodionov, D.S., de Suza Jr., P.A., Yen, A., Geliert, R., Evlanov, E.N., Zubkov, B., Foh, J., Bonnes, U., Kankeleit, E., Gütlich, P., Ming, D.W., Renz, F., Wdowiak, T., Squyres, S.W., Arvidson, R.E., 2004. Jarosite and hematite at Meridiani Planum from Opportunity's Mössbauer spectrometer. *Science* **306**, 1740–1745.

Lazaroff, N., Sigal, W., Wasserman, A., 1982. Iron oxidation and precipitation of ferric hydroxysulfates by resting *Thiobacillus ferrooxidans* cells. *Appl. Environ. Microbiol.* **43**, 924–938.

Lazaroff, N., Melanson, L., Lewis, E., Santoro, N., Pueschel, C., 1985. Scanning electron microscopy and infrared spectroscopy of iron sediments formed by *Thiobacillus ferrooxidans*. *Geomicrobiol. J.* **4**, 231–266.

Majzlan, J., Myneni, S.C.B., 2005. Speciation of iron and sulfate in acid waters: aqueous clusters to mineral precipitates. *Environ. Sci. Technol.* **39**, 188–194.

Nicomrat, D., Dick, W.A., Tuovinen, O.H., 2006a. Assessment of microbial community in a constructed wetland that receives acid coal mine drainage. *Microb. Ecol.* **51**, 83–89.

Nicomrat, D., Dick, W.A., Tuovinen, O.H., 2006b. Microbial populations identified by fluorescence in situ hybridization in a constructed wetland treating acid coal mine drainage. *J. Environ. Qual.* **35**, 1329–1337.

Niemelä, S.I., Riekkola-Vanhanen, M., Sivelä, C., Viguera, F., Tuovinen, O.H., 1994. Nutrient effect on the biological leaching of a black-schist ore. *Appl. Environ. Microbiol.* **60**, 1287–1291.

Odum, J.K., Hauff, P.L., Farrow, R.A., 1982. A new occurrence of ammoniojarosite in Buffalo, Wyoming. *Can. Mineral.* **20**, 91–95.

Olson, G.J., Brierley, J.A., Brierley, C.L., 2003. Bioleaching review part B. Progress in bioleaching: applications of microbial processes by the minerals industries. *Appl. Microbiol. Biotechnol.* **63**, 249–257.

Rohwerder, T., Gehrke, T., Kinzler, K., Sand, W., 2003. Bioleaching review part A: progress in bioleaching: fundamentals and mechanisms of bacterial metal sulfide oxidation. *Appl. Microbiol. Biotechnol.* **63**, 239–248.

Sasaki, K., 1997. Raman study of the microbially mediated dissolution of pyrite by *Thiobacillus ferrooxidans*. *Can. Mineral.* **35**, 999–1008.

Sasaki, K., Konno, H., 2000. Morphology of jarosite-group compounds precipitated from biologically and chemically oxidized Fe ions. *Can. Mineral.* **38**, 45–66.

Sasaki, K., Tsunekawa, M., Konno, H., 1995. Characterization of argentojarosite formed from biologically oxidized Fe^{3+} ions. *Can. Mineral.* **33**, 1311–1319.

Sasaki, K., Tanaike, O., Konno, H., 1998. Distinction of jarosite-group compounds by Raman spectroscopy. *Can. Mineral.* **36**, 1225–1235.

Smith, W.L., Lampert, J.E., 1973. Crystal data for ammoniojarosite. $NH_4Fe_3(OH)_6(SO_4)_2$. *J. Appl. Crystallogr.* **6**, 490.

Stoffregen, R.E., Alpers, C.N., Jambor, J.L., 2000. Alunite–jarosite crystallography, thermodynamics and geochronology. *Rev. Mineral. Geochem.* **40**, 453–479.

Vegard, L., Dale, H., 1928. Untersuchungen über Mischkristalle und Legierungen. *Z. Kristallogr. Kristallogeom. Kristallphys. Kristallchem.* **67**, 148–162.